UCRL-JC-109815

PCMDI
Program for Climate Model Diagnosis and Intercomparison

PCMDI Report No. 2

ANALYSIS OF THE TEMPORAL BEHAVIOR OF TROPICAL CONVECTION IN THE ECMWF MODEL

by

Julia M. Slingo[1], Kenneth R. Sperber[2], Jean-Jacques Morcrette[3]
and Gerald L. Potter[2]

[1]Department of Meteorology, University of Reading, Reading, England

[2]Program for Climate Model Diagnosis and Intercomparison
Lawrence Livermore National Laboratory, Livermore, CA, USA

[3]European Centre for Medium-Range Weather Forecasts, Reading, England

April 1992

PROGRAM FOR CLIMATE MODEL DIAGNOSIS AND INTERCOMPARISON
UNIVERSITY OF CALIFORNIA, LAWRENCE LIVERMORE NATIONAL LABORATORY
LIVERMORE, CA 94550

ABSTRACT

Extended (180-day) high resolution (T106) perpetual January and July integrations of the ECMWF model have been analyzed in terms of the spatial and temporal characteristics of the model's convective activity in the tropics. The model's outgoing longwave radiation (OLR) is used as a surrogate for convective activity, consistent with similar studies based on satellite observations. The 3-hourly temporal sampling is sufficient to allow diagnosis of intra- and interdiurnal variability; the length of the integrations is adequate for identifying lower frequency intraseasonal phenomena. Wherever possible, use is made of the results from surface or satellite observations of the temporal characteristics of convection to verify the model results.

At intradiurnal time scales, the model captures the amplitude and phase of the diurnal harmonic over both land and sea. The largest amplitudes occur over the summer continents, with contrasting phases of maximum OLR depending on the presence of convective activity. Over the oceans, the model show a coherent structure to the diurnal cycle associated with regions of convection.

Analysis of synoptic (2 to 10 days) and low frequency (greater than 10 days) variability shows that in many instances the model agrees well with observations. For both seasons, the model simulates westward moving phenomena over the oceans whose phase speed is reasonable. In July, these easterly waves display well-defined periodicities in agreement with observations, whilst in January they are more episodic. Low frequency variability is more prevalent in January, particularly over the convectively active regions of the eastern hemisphere. In general, this variability has a larger spatial scale than synoptic variability; its periodicities, some in excess of 30 days, are typical of intraseasonal time scales.

1. Introduction

It has been known for many years that tropical convection is highly variable both in space and time. Although, in a time mean sense, the intertropical convergence zone (ITCZ) appears as a smooth line of convection stretching across the equatorial oceans, it is, as satellite photographs show, built up of a large number of convective cells, some of which may be organized on the scale of a hundred kilometers or more. Studies based on conventional surface observations and on analyses of satellite data have revealed a myriad of time and space scales for convection. These range from the individual clouds and the cloud clusters associated, for example, with easterly waves, to the super clusters which often display eastward propagation characteristic of the intraseasonal oscillation. A recent paper by Lau et al. (1991) illustrates the coexistence of the different scales of organization, with westward moving cloud clusters embedded in an eastward moving ensemble of clusters.

The relationship between the time mean circulation and the time mean diabatic heating is reasonably well understood (e.g. Webster 1983), but the role of the transient component of the thermal forcing is less clear. However, the importance of organized convection in the excitation of planetary waves and possible teleconnections with the extra-tropics (e.g. Wallace and Gutzler 1981; Hoskins and Karoly 1981; Simmons 1982), the development and maintenance of equatorial waves (e.g. Nitta 1972; Gill 1980; Zangvil and Yanai 1981) and the propagation of these waves into the stratosphere (e.g. Yanai and Hayashi 1969; Holton 1972) has been demonstrated. Thus, whilst a general circulation model should be able to simulate with reasonable fidelity the mean radiation and cloud and precipitation fields, the model's ability to reproduce the appropriate time scales of these quantities may be equally important. If a model has the incorrect transient behavior of the latent heating then this may result in errors in the tropical circulation, extratropical teleconnection patterns and the development of equatorial waves and tides (e.g. Ferranti et al. 1990).

For a forecast model, the ability to represent equatorial waves may be crucial for predicting the development of tropical storms. For example, there is evidence that the number of typhoons in a given year may be related to the intensity of activity of the westward moving waves in the equatorial Pacific (Chang et al. 1970). Similarly, a climate model should be capable of representing the tropical transience if any conclusions regarding the incidence of tropical storms are to be made in the context of

climate change. In both respects, the transient behavior of the convection in the model and comparison with observations may provide useful information on the performance of the convective parameterization. An analysis of tropical disturbances in a general circulation model was made originally by Hayashi (1974), who identified the existence of a number of equatorial travelling waves. Since then, the simulation of transience in the tropics has received relatively little attention in comparison with the extratropical storm tracks.

This paper describes an analysis of the intradiurnal (≤1 day) and interdiurnal (>1 day) variations in convective activity in the tropics of the ECMWF model. The motivation for this study arose from the increasing number of papers which describe the observed variance for different time scales, based on data from geostationary satellites (e.g. Duvel 1988; Fu et al. 1990; Lau et al. 1991; Salby et al. 1991) and on analyses from numerical weather prediction models (e.g. Nitta et al. 1985; Lau and Lau 1990). These data have given an unprecedented view of the global characteristics of tropical convection. They offer a chance of relating disturbances in one part of the tropics with those in another; for example, the link between the West Pacific easterly waves, which have been studied extensively (e.g. Wallace and Chang 1969; Reed and Recker 1971; Liebmann and Hendon 1990), and those which occur in the East Pacific (Tai and Ogura 1987) might be clarified. The role of the extratropics in exciting equatorial waves has been the subject of a number of papers (e.g. Chang et al. 1979; Zangvil and Yanai 1980; Hartmann and Liebmann 1984). The global database offered by NWP analyses and satellite observations should allow further progress to be made in our understanding of the interaction between the tropics and the extratropics.

A study of the variance of tropical convection requires an integration of a general circulation model for at least one month and preferably much longer, with appropriate sampling of the diurnal cycle. This paper describes the results of integrations made with the ECMWF model at Lawrence Livermore National Laboratory as part of a cooperative research effort between these institutions. These integrations are ideally suited for this study, since radiation and surface hydrological parameters were archived eight times a day thus providing a good description of the diurnal cycle. The integrations were 180 days in length for perpetual January and July, long enough to allow analysis of both the high and low frequency variability of convection.

The geographical distribution of disturbances in the model is studied and their characteristics in terms of period and phase speed are assessed. The relationship

between disturbances in different regions of the tropics is considered, and the seasonal dependence of the results is also described. An important feature of this analysis is that the absolute value of a parameter need not be known or modelled with a high degree of accuracy, rather that the relative fluctuations be comparable with those observed from satellites. The time scales of these fluctuations should give insight into such phenomena as the diurnal cycle of cloudiness and/or precipitation (e.g. Meisner and Arkin 1987; Duvel 1988), the geographical and spatial structure of easterly waves (e.g. Duvel 1990) and the longer period variations in cloudiness associated with the intraseasonal oscillation (e.g. Rui and Wang 1990; Hendon and Liebmann 1990).

Section 2 gives details of the model and the integrations, and Section 3 describes the results of a spectral analysis of the variance in several frequency bands; a more detailed analysis of the spectra in certain regions and a comparison with observed spectra wherever possible is also presented. Examples of the propagation characteristics of the convective activity are shown. Since this paper is essentially an introductory description of the tropical variability in a general circulation model, Section 4 addresses a number of further issues, some of which are already under investigation.

2. Description of the model and integrations

The results described in this paper are from integrations using the version of the ECMWF model which was operational in July 1989 (i.e., cycle 32). Descriptions of the dynamical and physical parameterizations of the model are found in Simmons et al. (1988) and Tiedtke et al. (1988), respectively. The model has 19 levels in the vertical, represented by a hybrid coordinate. In the horizontal, the prognostic variables are represented by truncated series of spherical harmonics. In this study a resolution of T106 was used, representing triangular truncation retaining the first 106 spectral coefficients. Physical tendencies are calculated on a Gaussian collocation grid where the mesh size is 1.125°.

Important features of this version of the model are the convective and radiative parameterizations, both of which differ from those described in Tiedtke et al. (1988). Convective processes are parameterized using the mass flux scheme developed by Tiedtke (1989). The scheme represents various types of convection, from the penetrative convection maintained by large-scale convergence of moisture to the shallow convection such as tradewind cumuli, associated with suppressed conditions. The

radiation parameterization is described in Morcrette (1990, 1991a); its correction of known errors in the shortwave and longwave clear sky heating profiles gave much greater destabilization of the tropical atmosphere and, consequently, a much more vigorous hydrological cycle. The radiative properties of clouds were also modified such that the emissivities of tropical cirrus clouds were increased, resulting in a much improved simulation of the outgoing longwave radiation (Morcrette 1990).

The model includes a diurnal cycle with full radiation calculations being performed every 3 hours. In the intervening time, the radiation fields are updated every time step (900 seconds) using the instantaneous solar zenith angle in the shortwave and the instantaneous temperature profile in the longwave. The operational version of the ECMWF model performs the full radiation calculations on a reduced horizontal grid in order to limit the computation time. In the present integrations, however, where the radiative fluxes are of prime concern, the full radiation calculation is performed at every grid point.

The model was integrated for 180 days for perpetual January and July conditions using the climatological sea surface temperatures of Alexander and Mobley (1976). For both integrations, the instantaneous total and clear sky radiation fields were saved every 3 hours. The precipitation was accumulated and saved on a daily basis. All the results presented in the following section are based on days 11 to 180 from each integration. The first 10 days were discarded to eliminate most of the spin-up effects involving the adjustment of the model's atmospheric state to the imposed sea surface temperatures.

3. Simulated outgoing longwave radiation

a. *Time mean fields and total variance*

The method of analysis will primarily use the outgoing longwave radiation (OLR). This field was chosen because it closely matches the parameters, such as brightness temperature, typically used in satellite studies. These studies will constitute the main sources of information for comparing the model's variability with observations. Figure 1 shows the time averaged OLR over the tropical belt between 30° N and 30° S for both January and July. Contours of the time mean precipitation have been superimposed to show how well the model's OLR correlates with the convection. The close correspondence between the areas of precipitation and low values of

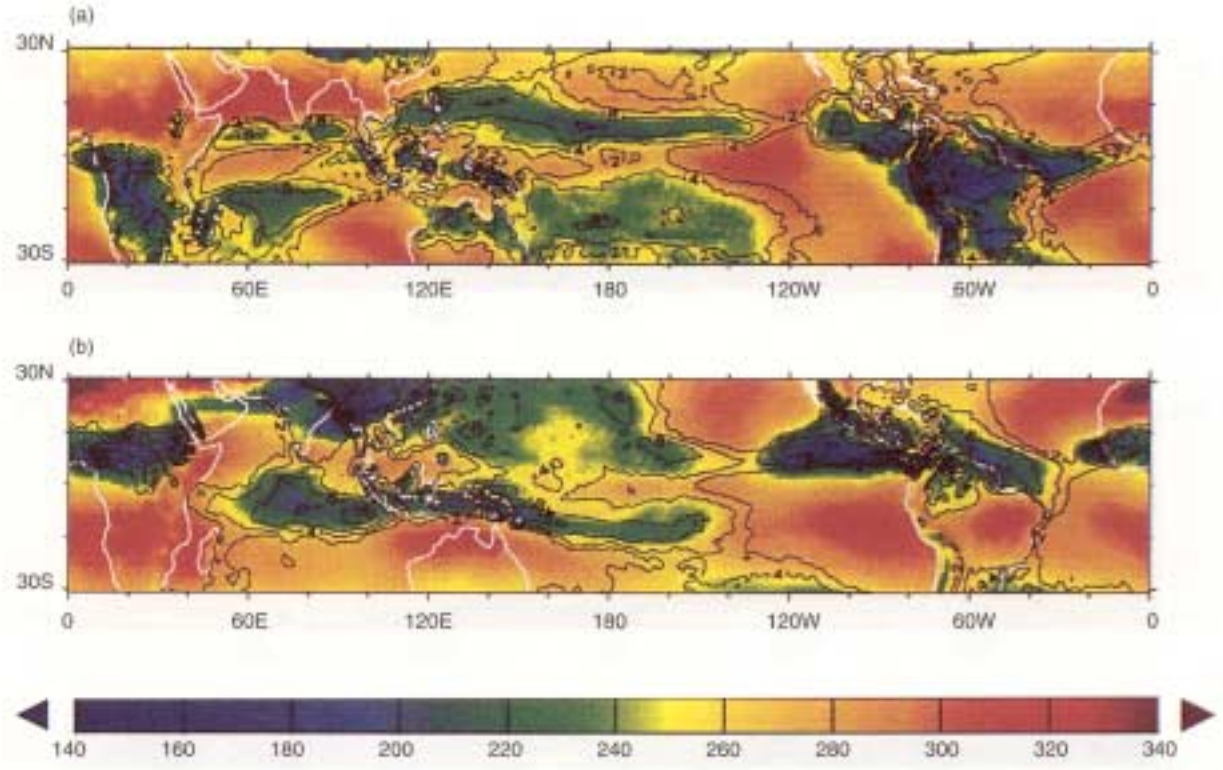

Fig. 1. Time mean OLR (W m^{-2}) and precipitation rate (mm day^{-1}) averaged between days 11 and 180 for (a) January, and (b) July.

OLR is not surprising since the cloud prediction is closely linked to the convection through the precipitation rate (Slingo 1987). For example, in regions of deep strong convection, the amount of model anvil cirrus cloud depends on the convective activity. Thus, the use of OLR as an indicator of convective activity in the model seems reasonable.

Figure 2 shows the OLR observed by ERBE for January 1986 and July 1985. Bearing in mind that the ERBE data are for a particular year and that there is interannual variability, the model has simulated many features of the observed tropical convection and its seasonal migration. The principal exception is over Indonesia and the West Pacific, where the model has produced a divided structure to the ITCZ, typical of the systematic error of this version of the ECMWF model (Miller et al. 1992) Compared with the ERBE data, the model has a tendency to give excessive maxima in the OLR over the subtropics. The model's clear sky longwave fluxes are also too high in these regions, compared with typical values from ERBE, indicating that the

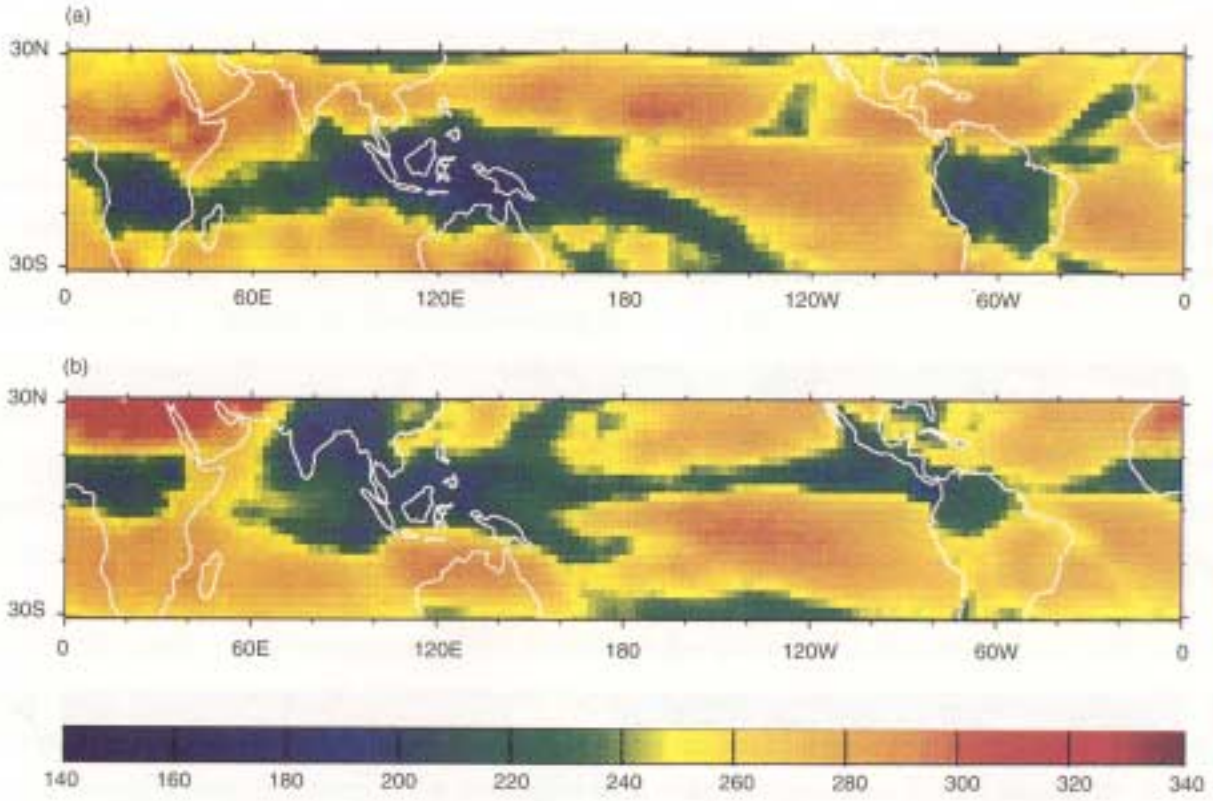

Fig. 2. Time mean OLR (W m^{-2}) from ERBE for (a) January 1986, and (b) July 1985.

anticyclones are too dry. In addition, the radiation scheme does not account for the effects of aerosols or trace gases which would also reduce the clear sky fluxes. Figures 1 and 2 also suggest that the minima in the simulated OLR are too low; this result can be attributed to the assumptions made to determine the liquid water content of the cirrus clouds and hence their emissivity. It now seems likely that the emissivities of these clouds are over-estimated (Morcrette, private communication).

The variance of the 3-hourly OLR against the time mean for days 11 to 180 for both seasons is shown in Fig. 3. Comparison with Fig. 1 indicates immediately that most of the convectively active regions, defined by high precipitation and low OLR, are also regions where the variance is large. Thus the model, far from producing more or less steady convection over the equatorial oceans, has a high degree of variability. A similar characteristic in the observations was noted by Salby et al. (1991) using satellite data. Exceptions seem to be the regions of very heavy rainfall over the East Pacific and off the coast of Pakistan in July, and over the Andes in January. The lack

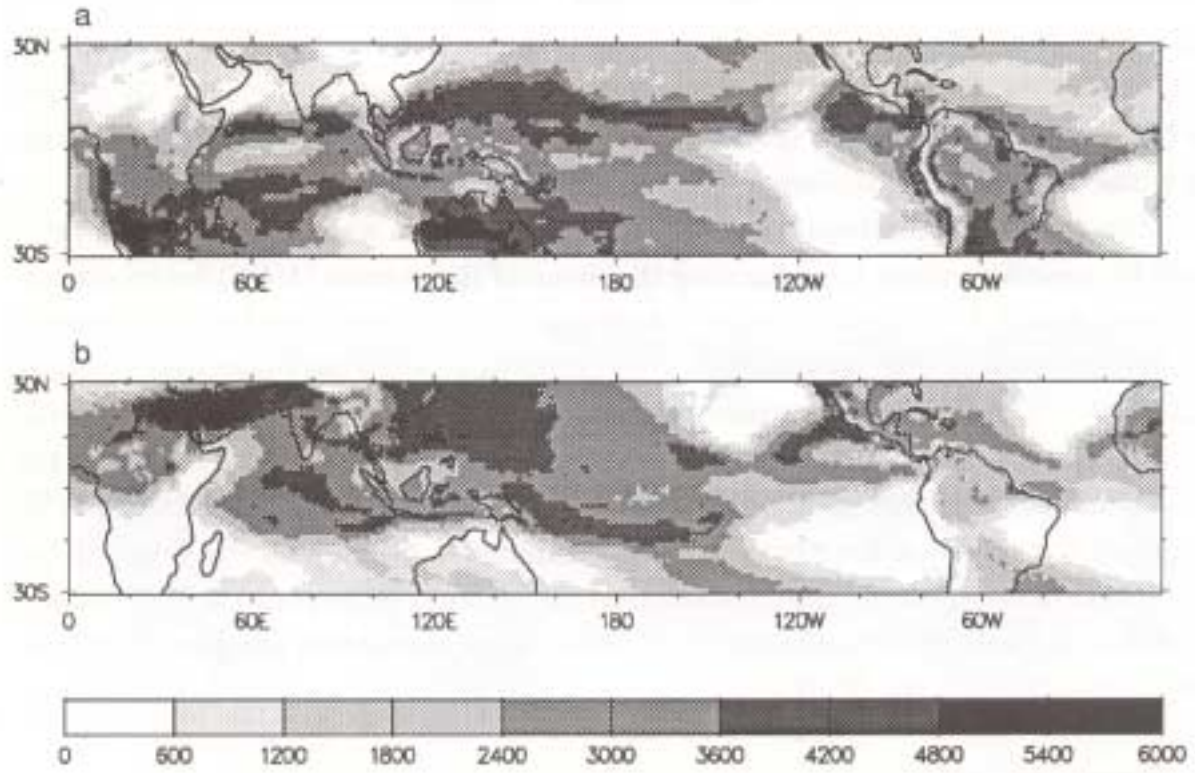

Fig. 3. Total variance $(W m^{-2})^2$ of the 3 hourly samples of OLR for days 11 to 180 for (a) January, and (b) July.

of variance over the Andes highlights typical problems with general circulation models in their treatment of steep orography. The Andes provide a region of continuous uplift with persistent precipitation occurring along their length. On either side of the mountain range the OLR is far more variable. Figure 3 also shows that the variance is large over some land areas where the mean OLR is high and the precipitation is near zero (e.g. Arabia in July, southern Australia in January). This reflects the large diurnal cycle in the land surface temperatures which will be discussed further in the next section.

Spectral analysis of the time series of the OLR was carried out to identify the time scales of the variability in the model's convection. At each grid point the long term mean was removed before calculating the power spectrum for days 11 to 180. The time series was not detrended so that the climate drift of the model may appear in the lowest frequency. To allow comparison with the observed spectral characteristics,

the spectrum at each grid point was averaged into three bands, following those used by Salby et al. (1991). The first band represents the intradiurnal variance (periods ≤1 day), whilst the other two isolate the synoptic (periods between 2 and 10 days) and the low frequency variability (periods >10 days). Both the variance and the percentage of the total variance in each spectral ban were computed.

The spectral characteristics of the model's convection were examined in greater detail for specific regions by computing the mean of the spectra (MOS) for an ensemble of grid points. In this case, the individual spectra were normalized to unit variance before the spatial averaging was done in a similar manner to that described by Salby et al. (1991). The fluctuations which behave coherently over the domain in question were identified by computing the area average time series of the OLR, after which the normalized spectrum was calculated, thus giving the spectrum of the mean (SOM). In each case, the red noise spectrum was also computed to provide an indication of the significance of the spectra. Ideally, statistical significance of the peaks should be computed, but this was problematic due to the difficulty of estimating the degrees of freedom, particularly for the MOS.

b. Diurnal variation

The variance of OLR associated with periods of less than or equal to one day (the intradiurnal variance) is shown in Fig. 4 for both seasons. Also shown is the percentage of the total variance explained by intradiurnal time scales. It should be noted that the intradiurnal variance includes not only the variance forced by the diurnal cycle of radiative heating, but also that associated with random short time scale fluctuations, such as squall lines. The greatest intradiurnal variance occurs over the summer continents, while over the oceans the variance is small. The percentage of the total variance (Figs. 4b and 4d) shows a similar picture, although over the winter continents, such as South Africa in July and North Africa and Arabia in January, almost all the total variance, albeit small, is explained by intradiurnal time scales. As noted earlier in Fig. 3, problems with the model's treatment of steep orography can be seen in January in the vicinity of the Andes (Figs. 4a and 4b). The variance to the west of South America appears to be largely explained by intradiurnal variability, possibly forced by that to the east of the Andes. To isolate that part of the intradiurnal variability which is directly linked to the response of the surface/atmosphere system to the diurnal cycle in the solar radiation, the coherent diurnal variation has been analyzed.

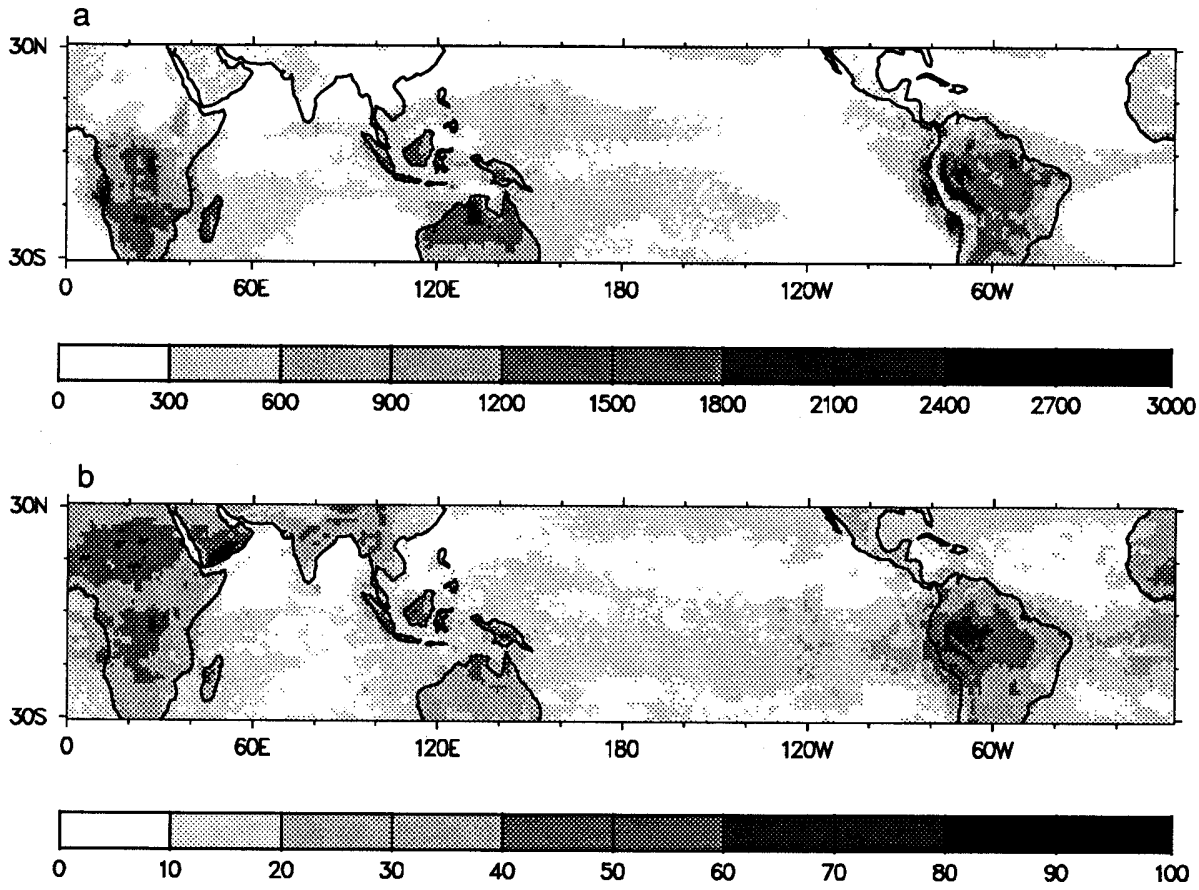

Fig. 4. Variance $(W\ m^{-2})^2$ and the percentage of the total variance of OLR associated with periods less than or equal to 1 day (i.e. intradiurnal variance). (a) and (b) are the actual and percentage OLR variances for January.

This was obtained by computing the time mean OLR for each of the eight times of day, separated by three hourly intervals. The standard deviation of the eight time mean values of OLR is equivalent to the coherent diurnal variation computed by Duvel (1988) using METEOSAT data. Harmonic analysis of the time series of eight OLR values was carried out and the phase and amplitude of the diurnal (first) harmonic has been plotted. The amplitude of the semi-diurnal (second) harmonic has also been considered, but was found to be much smaller than the diurnal harmonic. Comparison of the standard deviation of the eight OLR values with the amplitude of the diurnal harmonic shows that the diurnal harmonic accounts for at least 95% of the total coherent standard deviation in most circumstances.

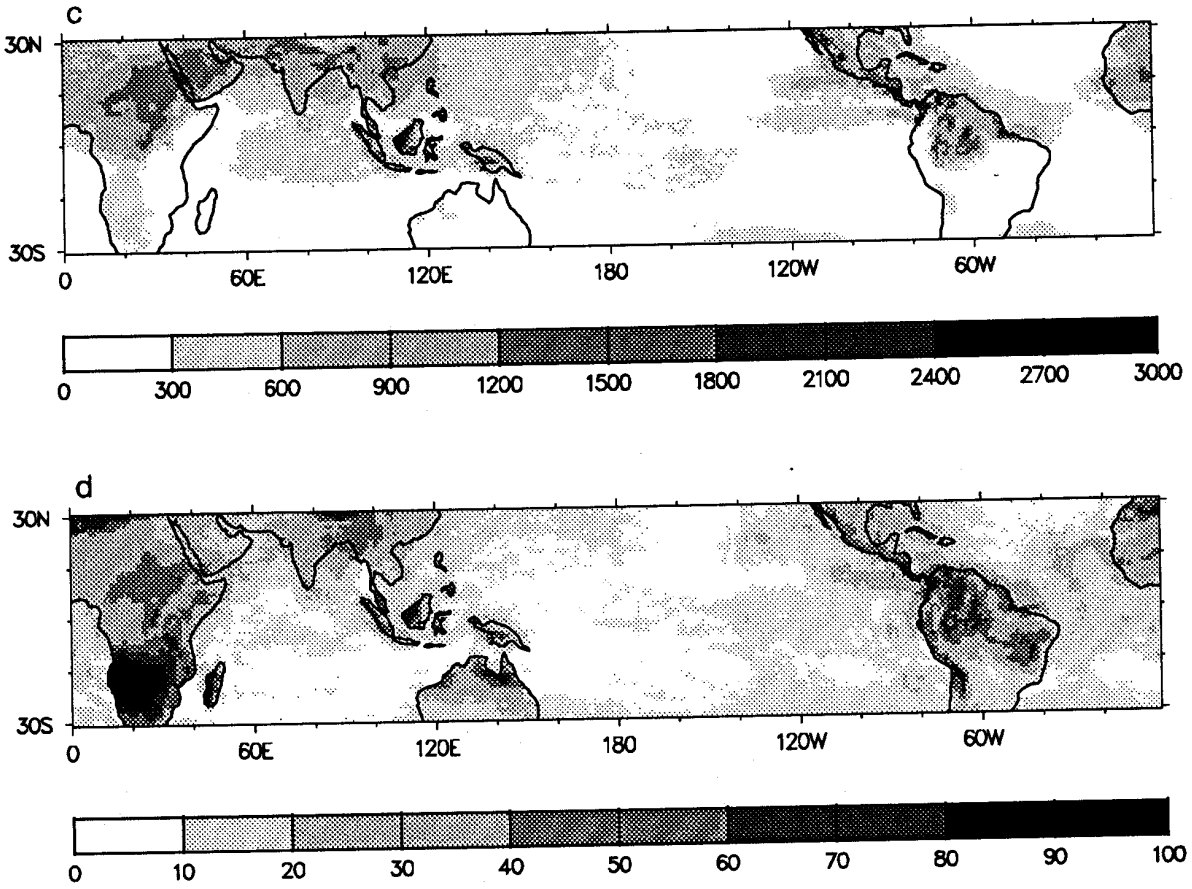

Fig. 4 (con't). (c) and (d) are the actual and percentage OLR variances for July.

Figure 5 shows the amplitude of the diurnal harmonic of OLR from the model for January and July. This can be compared with similar figures for the global tropics given by Hartmann and Recker (1986), based on data from four sun synchronous satellites during the period 1974 to 1983. Many of the detailed features in the observed amplitude of the diurnal harmonic have been reproduced by the model. As in Hartmann and Recker's results, the amplitude is largest over land. This is true both for regions of subsidence, e.g. South Africa in July, and for regions with deep convection, e.g. South America, characterized by low values of the time mean OLR (Fig. 1). The magnitude of the variation, in excess of 20 W m^{-2}, is in good agreement with the results of Hartmann and Recker (1986) and Minnis and Harrison (1984). This suggests that the model's convection scheme responds quite realistically to the diurnal cycle in

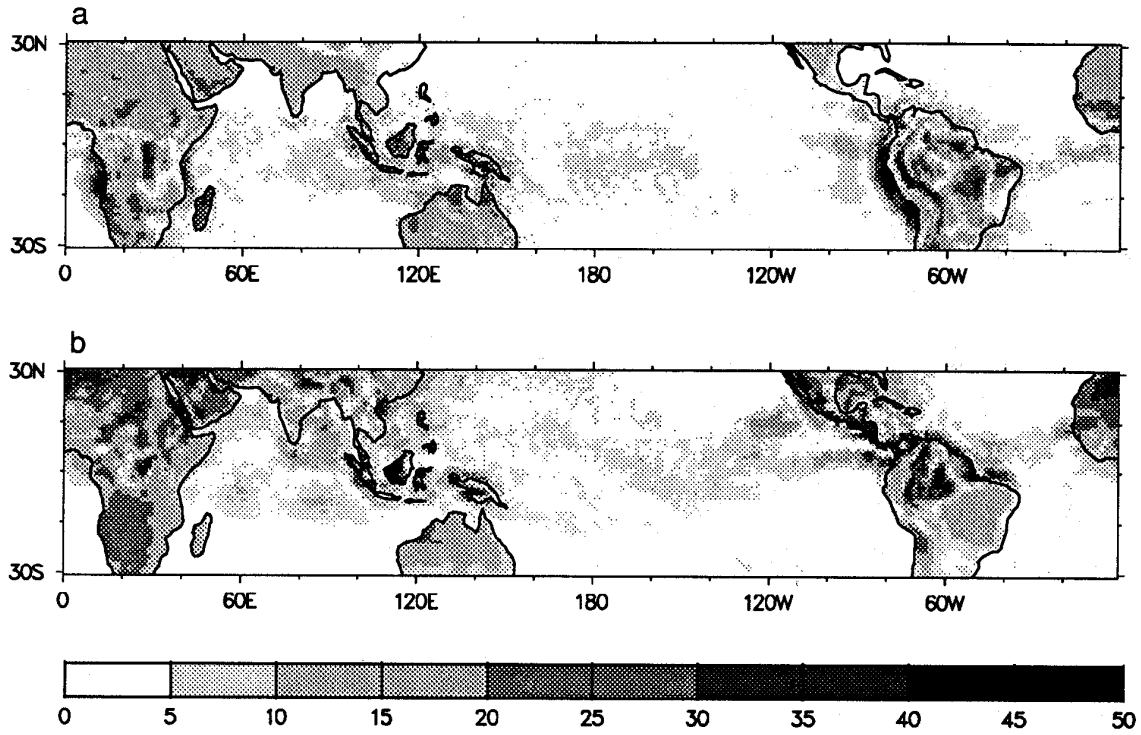

Fig. 5. Amplitude (W m^{-2}) of the diurnal harmonic for (a) January, and (b) July.

shortwave heating.

A striking feature of Fig. 5 is the well defined structure of the amplitude of the diurnal harmonic over the equatorial oceans. As noted by Hartmann and Recker (1986) and Meisner and Arkin (1987), this is most marked where convection is most well developed, such as the Atlantic ITCZ and over the East Pacific and Indian Oceans in July. The magnitude of the variability, in excess of 5 W m^{-2}, is in good agreement with the values obtained by Hartmann and Recker (1986). They attribute this variation to changes in convective cloudiness, much as was suggested earlier by Gray and Jacobson (1977). Slingo et al. (1987) noted a similar variation over the tropical oceans in the U.K. Meteorological Office general circulation model which, they were able to relate almost entirely to changes in cloud amount.

The phase of the diurnal (first) harmonic, depicting the local time of the maximum in the OLR, is plotted in Fig. 6 for both seasons. In comparison with Hartmann and Recker (1986), the results show many interesting similarities. Over clear sky

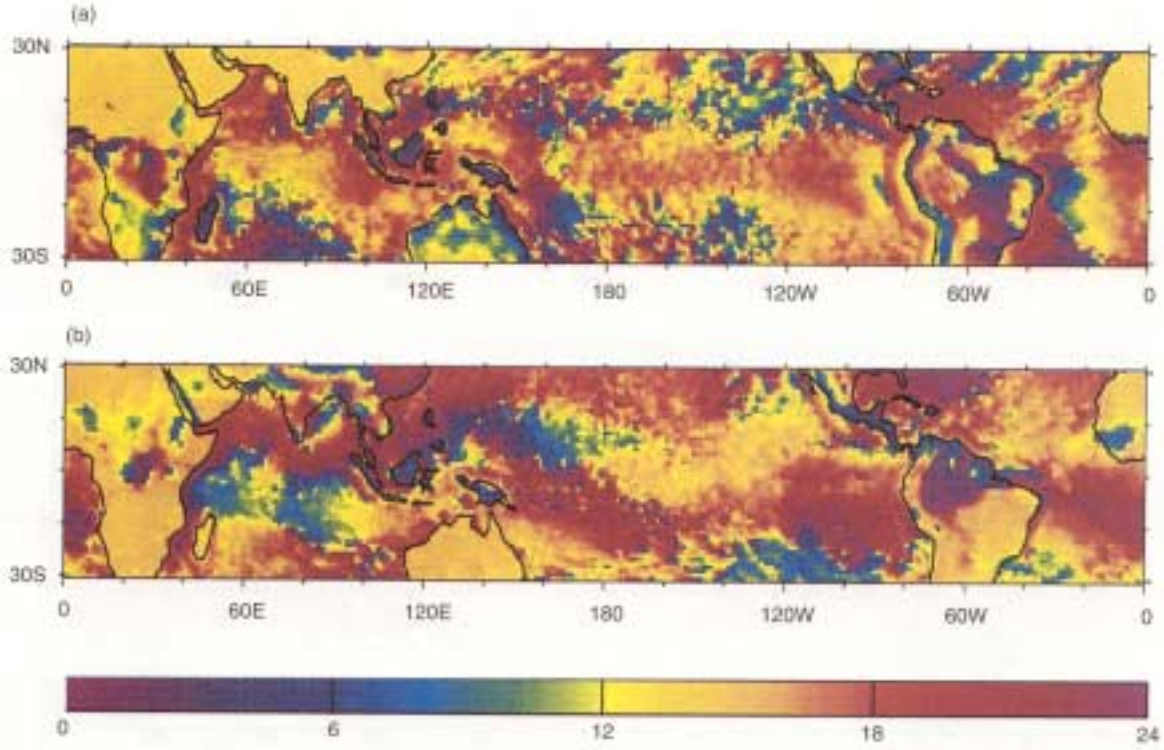

Fig. 6. Phase (local time of the maximum OLR) of the diurnal harmonic for (a) January, and (b) July.

land areas (characterized by high values of OLR in Fig. 1), the maximum in the OLR occurs consistently in the early to mid-afternoon, after the peak in the shortwave heating. This is in agreement with the ISCCP data as analyzed by Morcrette (1991), which show a peak emittance at 1500 LST. In contrast, the regions of deep convection (i.e. low OLR), such as South America and Indonesia, show that the maximum in the OLR occurs near midnight, implying that convective activity is greatest during the day. Again, this is consistent with the results of Hartmann and Recker (1986) and Meisner and Arkin (1987).

It is interesting to note that for extensive areas of the equatorial Pacific and the Indian Oceans where convection is present but not particularly strong (e.g. East Pacific in July, South Pacific convergence zone (SPCZ) in January), the phase of the diurnal harmonic indicates a near noon maximum in the OLR (Fig. 6). This is particularly marked where the amplitude of the diurnal harmonic is in excess of 5 W m^{-2} (Fig. 5). Hartmann and Recker (1986) note a similar phase in regions where oceanic convection occurred but is not particularly intense, and comment that this

result is consistent with the daytime minimum in precipitation observed at islands along the SPCZ (e.g. Gray and Jacobson 1977; Albright et al. 1985).

c. *Interdiurnal variability*

In this section, the synoptic and low frequency variability in the model's convective activity is analyzed for each season. Hovmoller (longitude/time) diagrams are used to identify the coherent nature of the variance and also to identify the propagation characteristics of individual events.

January

Figure 7 shows the variance associated with periods between 2 and 10 days (synoptic) and greater than 10 days (low frequency) for January. As expected, over the oceans most of the variability is associated with interdiurnal time scales compared with the land areas where it is mostly forced by the diurnal cycle in surface radiative heating. There are few observational data available for comparison mainly because most studies of equatorial transience have tended to concentrate on the northern summer. However, Salby et al. (1991) show similar figures for the transition season (August to December). Bearing in mind the differences in the time mean state, the partitioning of the variance within the various frequency bands has been simulated reasonably well by the model. The dominance of the synoptic scale variability (2 to 10 days) west of the dateline and extending down into the SPCZ can be clearly seen. Whereas the results of Salby et al. (1991) suggest a clear distinction between the synoptic and low frequency variability, particularly over the Indian Ocean and subcontinent and the equatorial Pacific, this is less apparent in the model. However, this may be due to the different seasons used for the analysis, and to the fact that their results are for a specific year and there may be some interannual variability. Clearly, more information on the observed variance over a number of years is required before any definite conclusions on this aspect of the model's performance can be made.

The percentage of the total variance explained by interdiurnal time scales (not shown) gives a slightly different view of the model's variability. Areas where the total variance is small but where a particular temporal behavior is large are emphasized by this approach. For example, over 50% of the total variance over the southeast Pacific and the Atlantic, north of the ITCZ, is explained by low frequency variability. This is a region of subsidence, and thus the variability is likely to be associated with

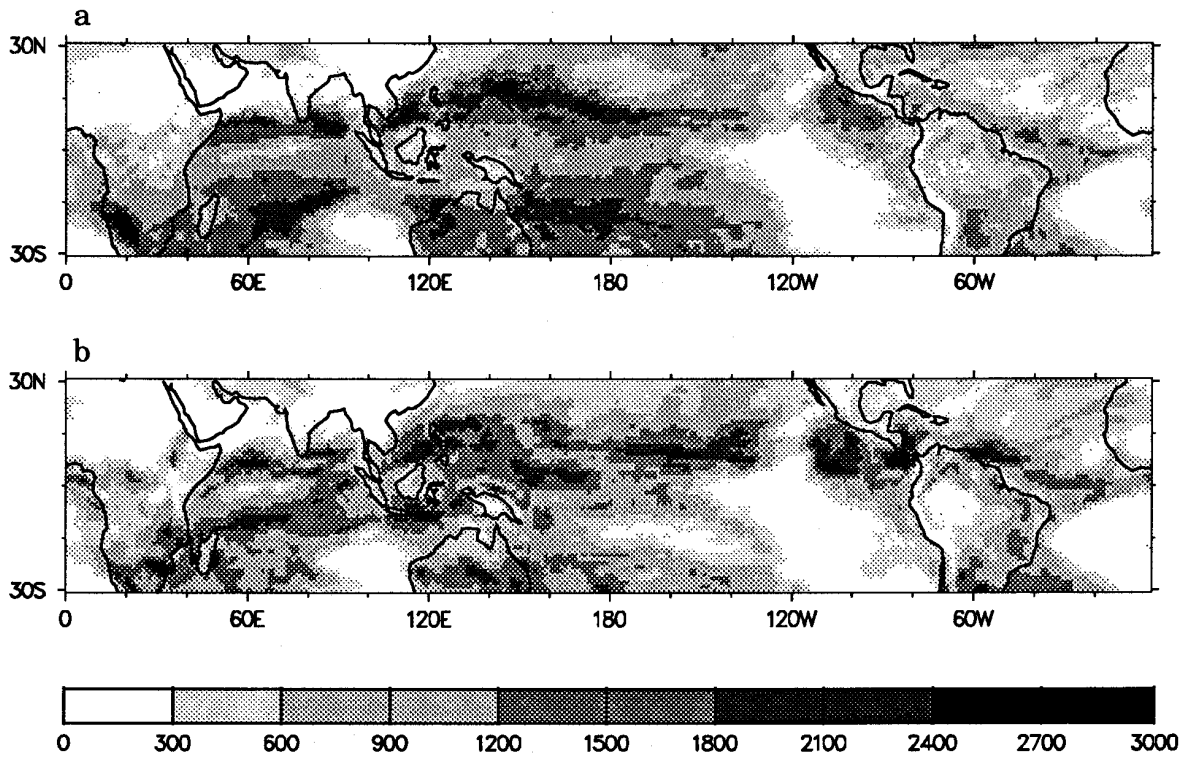

Fig. 7. Total variance $(W\ m^{-2})^2$ for January explained by (a) frequencies between 2 and 10 days, and (b) frequencies greater than 10 days.

fluctuations in atmospheric water vapor or low cloud amounts. This is consistent with the results of Duvel (1988), in which he noted that the METEOSAT water vapor channel data suggested a transition from short time scales in convergence areas to long time scales in subsidence areas. He related this long period variability in subsidence regions to changes in mid-tropospheric water vapor, associated with perturbations in the position of the subtropical jet which introduce differing air masses.

The results given in Fig. 7 suggest that the model is capable of reproducing the interdiurnal variability with some success. But what form does this variability take, and is it associated with any coherent propagating waves? Figure 8 shows a Hovmoller diagram of the OLR along 7° N for days 11 to 180. This latitude was chosen because it is roughly coincident with the maximum in the total variance across the Pacific Ocean (Fig. 3a). All scales of variability can be seen. The diurnal cycle in the land surface temperatures is evident over Africa between 0° and 30° E, as is the daily

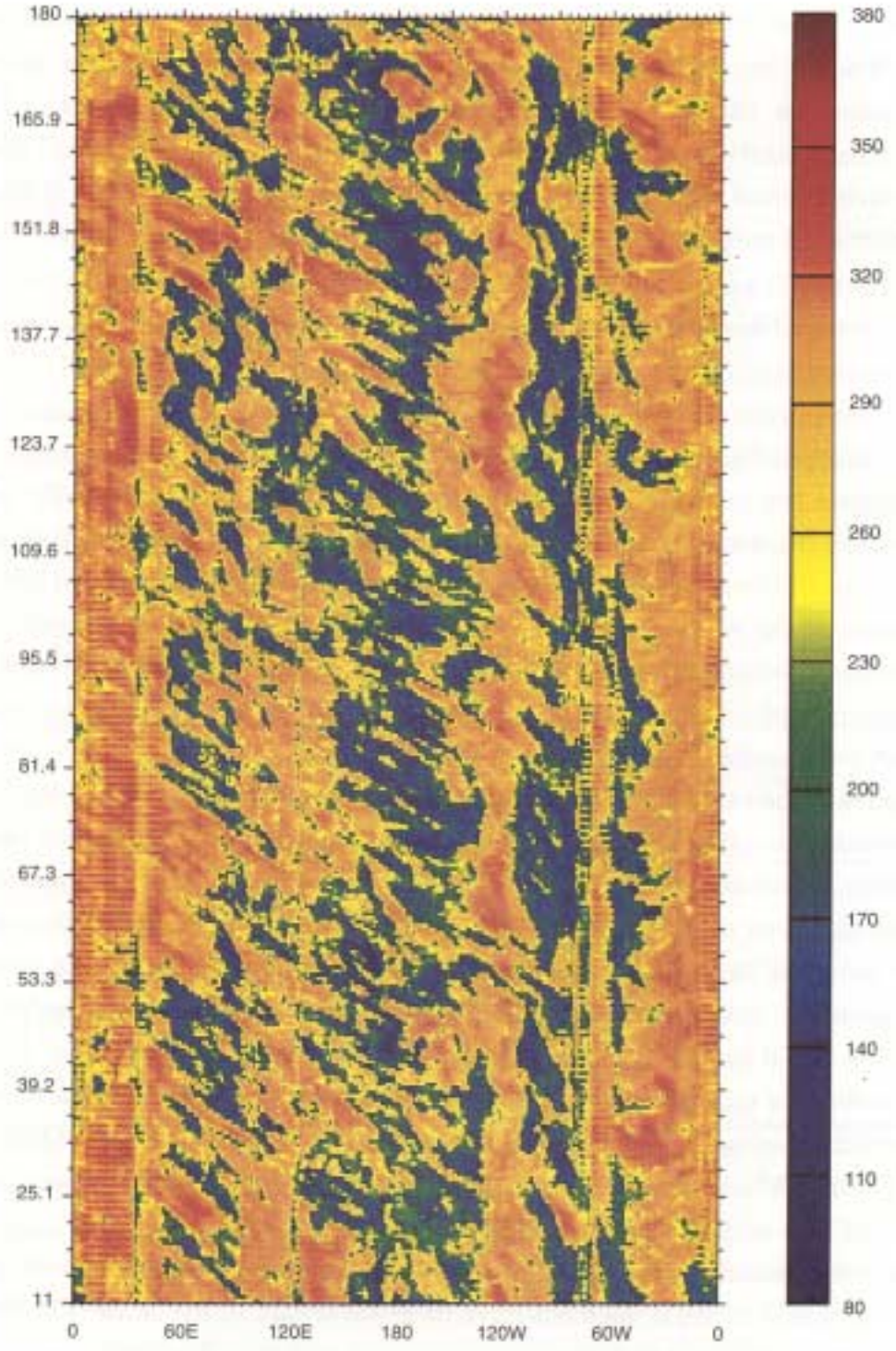

Fig. 8. Hovmoller diagram for days 11 to 180 of the OLR (W m^{-2}) along 7.3° N for January.

variation in convective activity over Central America (near 75° W) and Indonesia. Over the Pacific and Indian Oceans, westward moving features can be identified. In certain instances, there is some indication from Fig. 8 that the waves in the Indian Ocean are continuations of those in the Pacific Ocean. The phase speed of these waves is quite variable and probably reflects the variation in the wind speed at the steering level. Estimated subjectively for this latitude, the phase speeds lie between 10 and 14 m s^{-1} (7° to 11° per day) for the Pacific waves and between 5 and 11 m s^{-1} (4° to 8° per day) for those over the Indian Ocean. These speeds are all within the observed values for westward moving waves near the equator (e.g. Saha et el. 1981).

No clear periodicity with time is evident for the propagating features seen in Fig. 8. At this latitude the variability in the OLR seems to be more episodic than periodic. To investigate the periodicity of the variance of the OLR further, specific areas were chosen where the interdiurnal variability is large. Plots of the mean of the spectra and the spectrum of the mean were made, as described earlier. Consistent with the episodic nature of the waves in Fig. 8, very few of the spectra showed specific periodicities at synoptic frequencies between 2 and 10 days. In most, the spectrum was little different from red noise (i.e. a continuous increase in power with increasing periodicity), apart from some peaks at much lower frequencies.

Figure 9 shows spectra (MOS and SOM) for three regions in the Pacific and Indian Oceans. The solid lines represent the actual spectra, and the dashed lines the red noise spectrum, as described earlier. The mean of the spectra (MOS; Figs. 9a, c and e) show that all three regions are dominated by low frequency peaks, representing periodicities between 15 and 60 days. Those in excess of 20 days appear to be associated with large-scale structures, since they also dominate in the spectrum of the mean (SOM; Figs. 9b, d and f). Such large-scale low frequency variability in the OLR has been observed in association with the intraseasonal oscillation (e.g. Lau and Chan 1985), which displays a slow eastward propagation from the Indian Ocean into the central Pacific. Whether these long periodicities in the model's OLR are indeed representative of this oscillation is a subject for future research.

The pronounced peak at 15 days in the MOS over the West Pacific (Fig. 9a) is an interesting result. Since it does not have its counterpart in the SOM (Fig. 9b) it would appear to be a phenomenon whose spatial scale is less than the area of averaging. Lau et al. (1991), in a study of geostationary satellite data from December 1978 to February 1979, noted that 10- to 15-day periodicities in the convective activity were quite

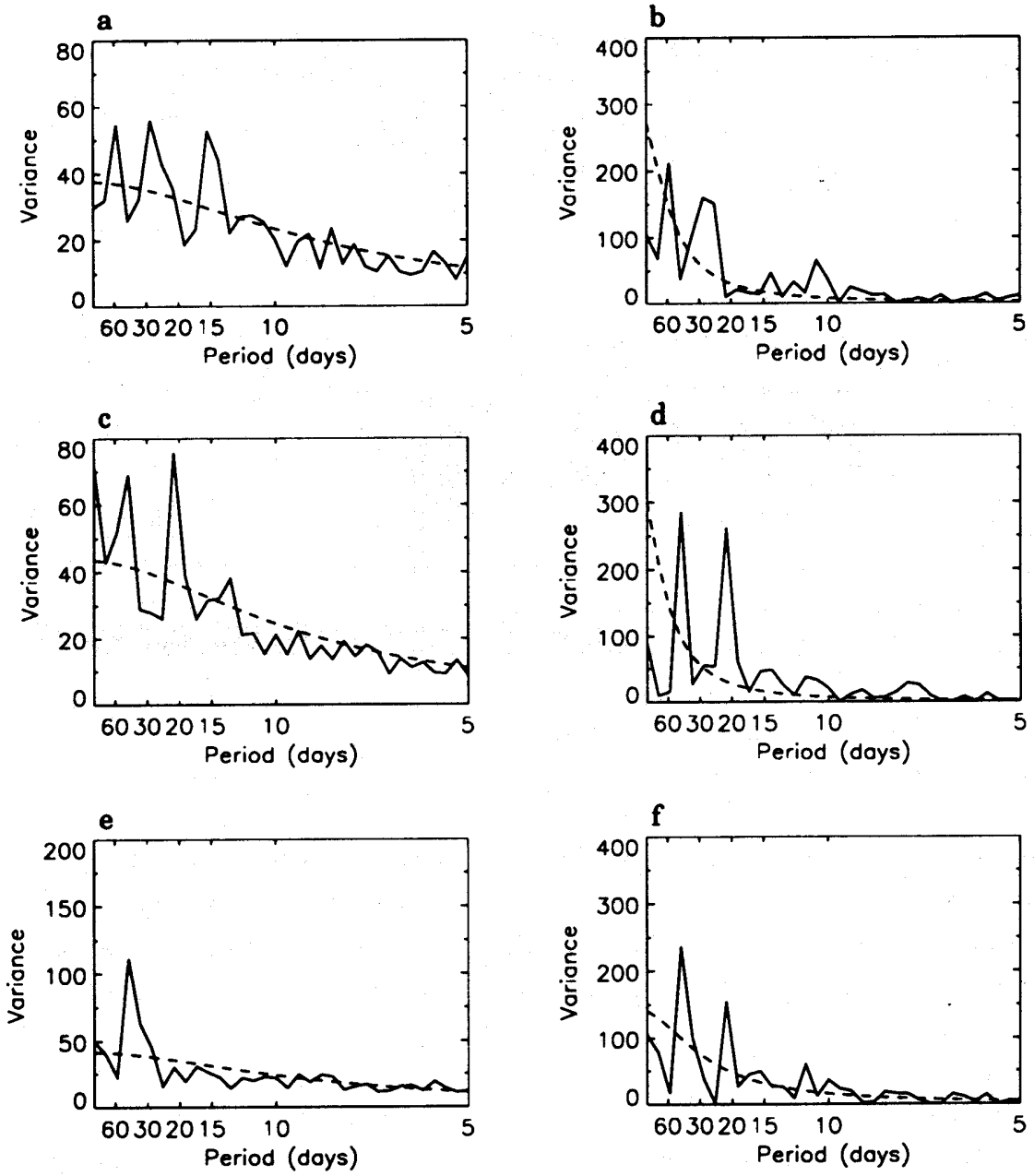

Fig. 9. Mean of the spectra (MOS) and spectrum of the mean (SOM) for days 11 to 180 for January. (a) MOS and (b) SOM for west Pacific (120° E - 150° E, 10° N - 20° N), (c) MOS and (d) SOM for central/east Pacific (180° W - 150° W, 5° N - 15° N), (e) MOS and (f) SOM for Indian Ocean (55° E - 95° E, 0° - 10° N). Solid lines are the actual spectra and dashed lines are the red noise spectra.

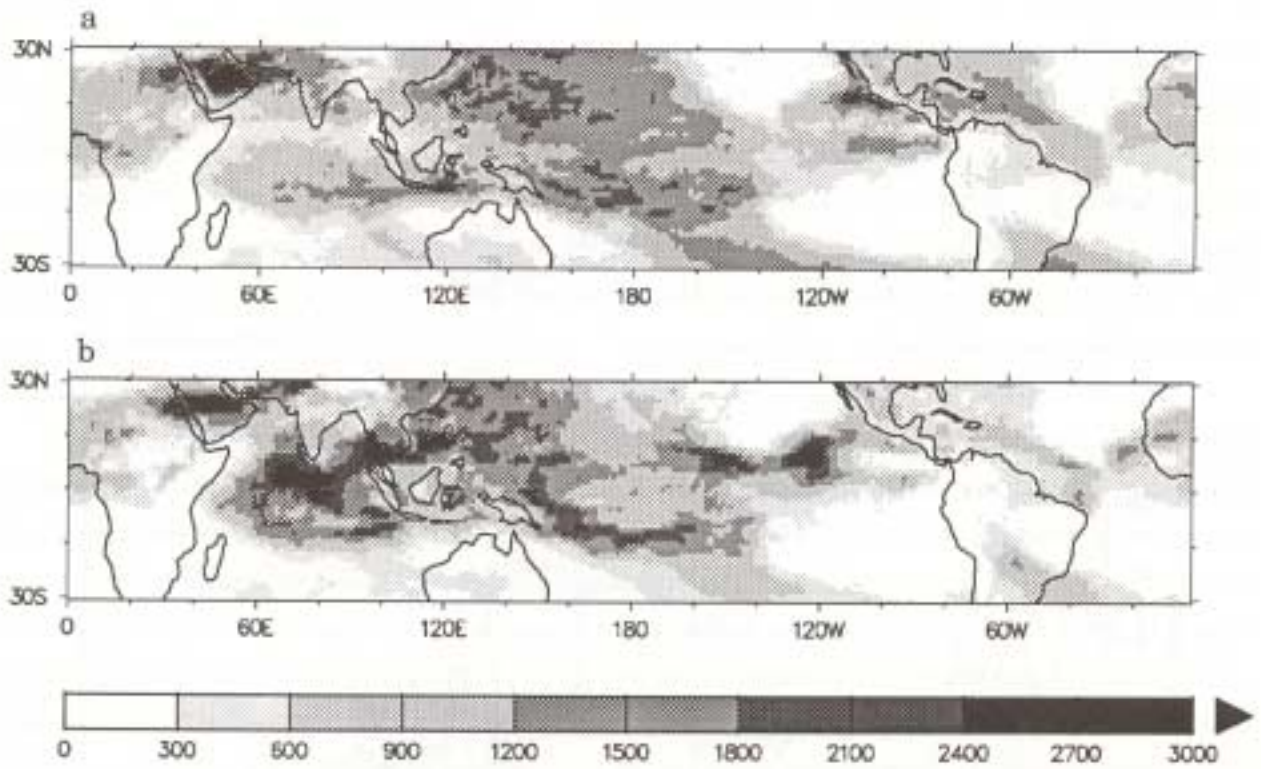

Fig. 10. Total variance $(W\ m^{-2})^2$ for July explained by (a) frequencies between 2 and 10 days, and (b) frequencies greater than 10 days.

dominant over the central and west Pacific, and appeared to be embedded in lower frequency variations associated with 30- to 60-day oscillations. The spectra shown in Figs. 9a and 9b for the west Pacific also indicate the coexistence of these periodicities in the model and a more detailed examination of their relationship is planned.

July

The partitioning of the total variance between synoptic and low frequencies for July is shown in Fig. 10. As with January, most of the interdiurnal variability occurs over the oceans, although considerable power is seen for periods between 2 and 10 days over Arabia. The distinction between the synoptic and low frequency variability is clearer in July, particularly over the Indian Ocean, consistent with the results of Salby et al. (1991). The tendency for long period variability to dominate in the Indian Ocean is also seen in the study by Nitta et al. (1985) for northern summer of the FGGE year. Quantitatively, it is hard to verify the level of activity in the model as

depicted by the OLR field. Comparison with the results of Nitta et al. (1985) suggests that it is too large over the west Pacific. This is consistent with the upper level clouds being radiatively too active in the model (Morcrette 1991). Over the Atlantic and equatorial Africa the variances associated with synoptic frequencies are nearer the values reported by Nitta et al. (1985). However, it should be noted that the satellite data used in their study had a horizontal resolution of 2.5° with less temporal sampling, so that a direct comparison with the model results may not be appropriate.

Over the east Pacific the variance is predominantly in the synoptic frequencies, with a transition to lower frequencies farther west. The dominance of synoptic frequencies off the American coast is supported by the studies of FGGE data by Tai and Ogura (1987) and Nitta et al. (1985), but the large low frequency variance between 120° W and 150° W is not present in their results. Again the question of interannual variability should be raised, since their results apply only to 1979. The percentages of the total variance explained by interdiurnal time scales (not shown) indicate that in the deep tropics the distributions are very similar to those for the actual variances (Fig. 10). However, in the subtropics poleward of 20°, where the total variance is not as large, synoptic frequencies explain a high percentage of the variance, possibly associated with the effects of mid-latitude disturbances.

The Hovmoller diagram of the OLR along 7° N for days 11 to 180 is shown in Fig. 11. As for January, the regimes of diurnal variability over the continents and interdiurnal variability over the oceans can be seen. Over the Indian Ocean the apparent cessation of convection after 50 days is related to a latitudinal shift in activity as the split in the ITCZ noted in Fig. 1b develops. Both the Pacific and Atlantic Oceans show westward moving features which display long period variability in their activity. For example, over the central Pacific, the disturbances are clearer in the first half of the integration, whilst over Africa and the Atlantic the easterly waves are extremely well defined during the last 60 days. Similarly, the highly periodic waves in the east Pacific are most prevalent between days 60 and 120. Reasons for this long term modulation in wave activity are unclear at this stage. However, this result suggests that an understanding of the variance within the model, and perhaps also the real atmosphere, requires long time samples.

Estimated subjectively from Fig. 11, the features in the central and west Pacific have a phase speed near 8 m s^{-1}, consistent with observed values of 9 m s^{-1} quoted by

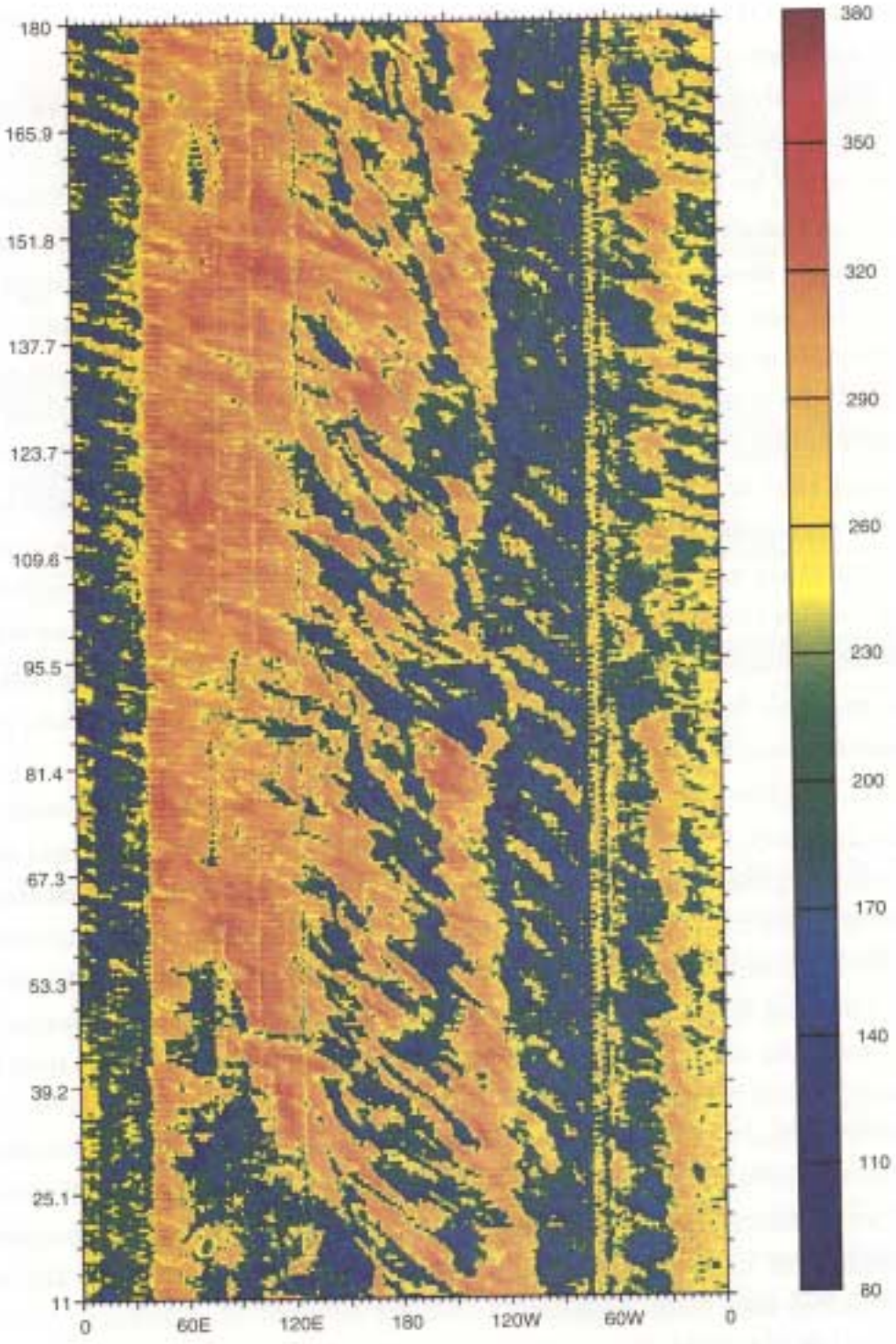

Fig. 11. Hovmoller diagram for days 11 to 180 of the OLR (W m^{-2}) along 7.3° N for July.

Reed and Recker (1971) for easterly waves diagnosed west of the dateline. The phase speed of the simulated Pacific waves is slower in July than in January. If the steering level of these waves is in the lower troposphere, then this result is consistent with the weaker low level easterlies in July. The highly periodic disturbances in the east Pacific have a slightly slower phase speed of between 6 and 7 m s^{-1}. This is in excellent agreement with the values quoted by Tai and Ogura (1987) based on FGGE data. The relationship between the waves in the central and west Pacific and those in the east Pacific is unclear from Fig. 11. The OLR represents only the cloud field whereas the wave may still be present in the wind fields. Clearly, further study is necessary to clarify this point. However, Fig. 11 does show that different periodicities exist in the two regions so that if there is a connection, some sort of selection process takes place to change the highly periodic nature of the OLR in the east Pacific to the more episodic nature of the convection farther west. The same conclusion can also be drawn over the Atlantic, where the model shows highly periodic waves developing over Africa and propagating into the Atlantic, but an episodic character to the convection over the Caribbean.

The change in the temporal characteristics of the disturbances as they propagate across the Pacific is evident also in the mean of the spectra for specific regions. Figure 12 shows the spectra for days 61 to 120, when the east Pacific waves are most prevalent (Fig. 11), for three areas over the east, central and west Pacific, respectively. Over the east Pacific (Fig. 12a) a pronounced peak near 7 days is seen. This is in excellent agreement with the observed spectra for this region based on either OLR or lower tropospheric meridional wind anomalies (Tai and Ogura 1987; Nitta et al. 1985). As suggested by the Hovmoller diagram (Fig. 11), this periodicity is disrupted farther west and the spectrum for a region over the central Pacific (Fig. 12b) shows no preferred peaks. Both Tai and Ogura (1987) and Nitta et al. (1985) noted a marked reduction in the power of the synoptic waves in the central Pacific, consistent with the model results, although their spectra suggest a very weak peak at higher frequencies between 2 and 4 days. However, their analysis is based on the lower tropospheric meridional wind anomalies, and it is possible for a wave to exist without a signature being seen in the OLR.

The mean of the spectra for an area over the west Pacific (Fig. 12c) shows no evidence of spectral peaks at synoptic frequencies, but a pronounced peak between 10 and 15 days. Consistent with the Hovmoller diagram (Fig. 11), there is little evidence

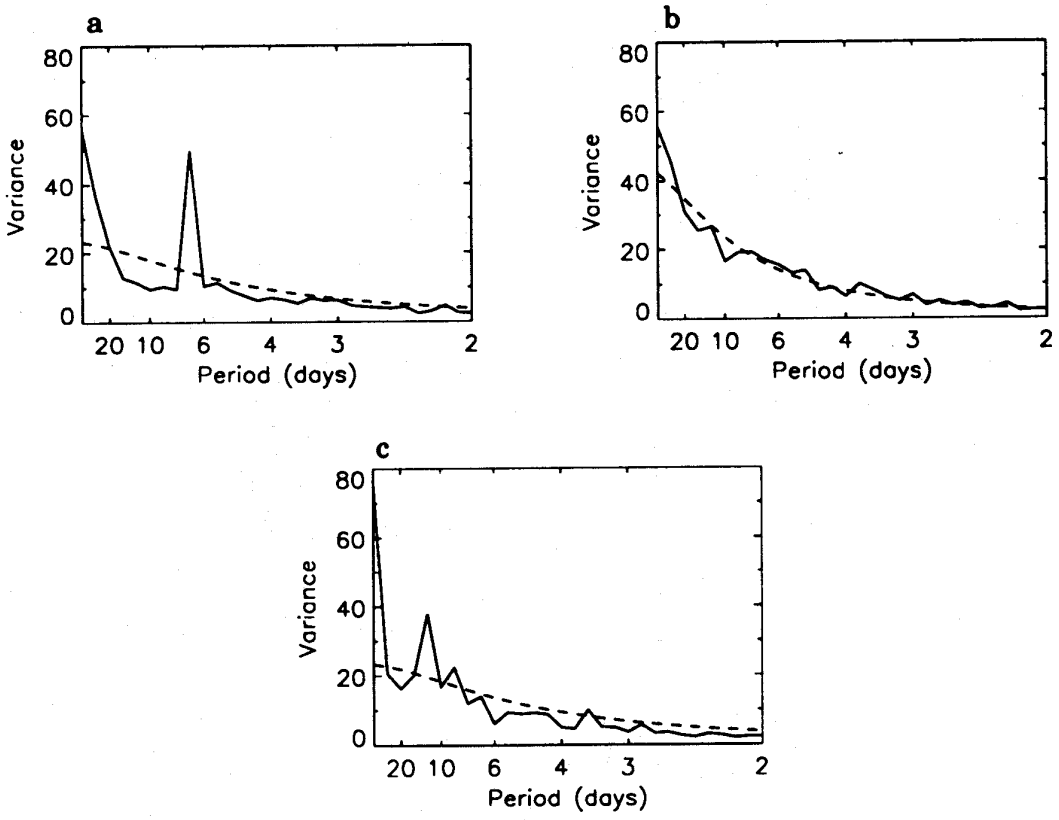

Fig. 12. Mean of the spectra for days 61 to 120 for July, for areas over (a) east Pacific (130° W - 100° W, 5° N - 20° N), (b) central Pacific (160° E - 140° W, 0° - 15° N), and (c) west Pacific/Indonesia (110° E - 130° E, 5° N - 20° N).

that the highly periodic waves of the East Pacific preserve their temporal characteristics through to the West Pacific. The dominance of lower frequencies in this region is supported by the analyses of FGGE data, although there is also evidence of the coexistence of shorter period synoptic frequencies. For example, at 7.5° N, Tai and Ogura (1987) show a broad peak in the power spectrum between about 4 days and in excess of 10 days, with the maximum power occurring near 6 days at 140° E. Farther west near 120° E this translates into a spectral peak between 10 and 15 days, similar to the model results. Nitta et al. (1985) also show very mixed periodicities in this region, with a 6-day wave dominating near 10° N but peaks at 4 and 10 days farther north and west.

During the last 60 days of the integration, the easterly waves over the Atlantic

and African sector are particularly regular (Fig. 11). The initiation of these waves occurs near 40° E over the Ethiopian Highlands, farther east than is generally observed. Despite the sparcity of surface data over East Africa, the source region of easterly waves is thought to lie between 15° E and 30° E (e.g. Burpee 1972, 1974; Reed et al. 1987). In the model these waves propagate rapidly westward across Africa and into the Atlantic, where, in terms of convective activity, they appear to dissipate between 20° W and 30° W. Over the west Atlantic the convection appears to be associated with lower frequency and longer lasting events which, in some instances, may be related to the waves farther east, although a comprehensive study of the wind fields would be required to clarify this point.

As is evident from Fig. 11, the phase speed of the model's African waves is almost twice the observed speed of near 8 m s^{-1}. A possible explanation for this discrepancy could lie in integrating a model in perpetual mode. As Zwiers and Boer (1987) note, the model can develop excessive contrasts between land and ocean, particularly in July, which may result in an unrealistic strengthening of the African easterly jet. Whilst a perpetual mode integration has advantages for frequency analysis, future studies should concentrate on the results from a multiyear seasonal cycle integration.

The mean of the spectra for regions over East Africa, the central Atlantic and the Caribbean are shown in Fig. 13. Consistent with the Hovmoller diagrams, the spectra for East Africa and the Atlantic (Figs. 13a and 13b) show a pronounced peak at 3.5 days, with an indication that the convection intensifies as the wave moves to the west. This periodicity is in excellent agreement with the observed frequency of African easterly waves from both GATE (Reed et al. 1977) and FGGE data (Nitta et al. 1985). Over the Caribbean (Fig. 13c) the spectrum is much noisier and, whilst the model still seems to preserve the 3.5-day periodicity, it coexists with a number of lower frequencies. Nitta et al. (1985) also show a shift to longer periods over the Caribbean, but in their case only to 6 days. Again, there is no information on interannual variability with which to assess the generality of their result. The results of the spectral analysis for regions over the Pacific and Atlantic sectors indicate that the dominant period of the variability lengthens towards the western part of each ocean. A similar characteristic was noted by Lau and Lau (1990) in their study of tropical disturbances using ECMWF analyses for the northern summer months.

Lau et al. (1991) have reported on the apparent coexistence of various scales of

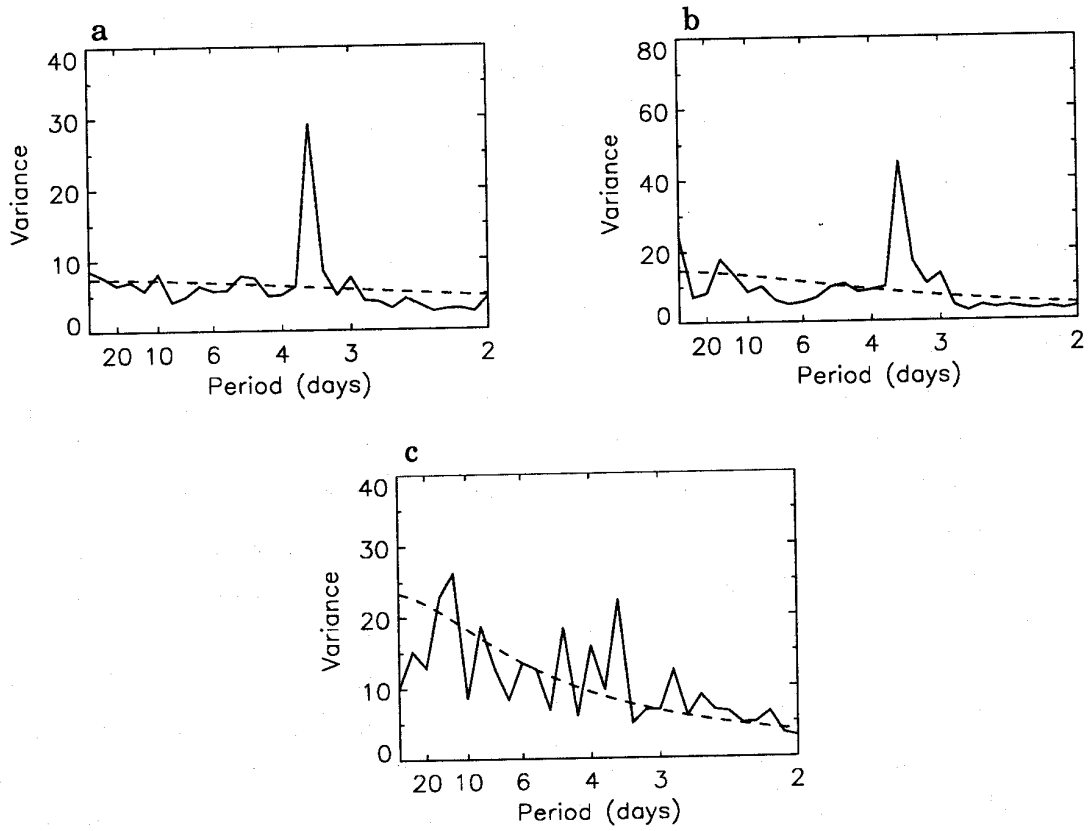

Fig. 13. Mean of the spectra for days 121 to 180 for July, for areas over (a) East Africa (20° E - 40° E, 5° N - 20° N), (b) central Atlantic (30° W - 0°, 5° N - 15° N), and (c) Caribbean (80° W - 50° W, 10° N - 25° N).

convection in the equatorial Pacific. They noted that westward moving cloud clusters at synoptic frequencies were often embedded in a much lower frequency eastward moving phenomenon which they classified as a super cloud cluster. In the model an example of the mean of the spectra (MOS) and the spectrum of the mean (SOM) for a region of the SPCZ shows an interesting difference between the spatial scales of the periodicity which might be indicative of the phenomenon described by Lau et al. (1991). The MOS (Fig. 14a) has a variety of peaks at synoptic and low frequencies with little distinction from red noise. In contrast, however, the SOM for that region (Fig. 14b) has a pronounced peak at 15 days. This suggests that, over a large spatial scale, there is a coherent low frequency oscillation of the area averaged OLR which is obscured in the mean of the spectra by a variety of smaller scale events of differing

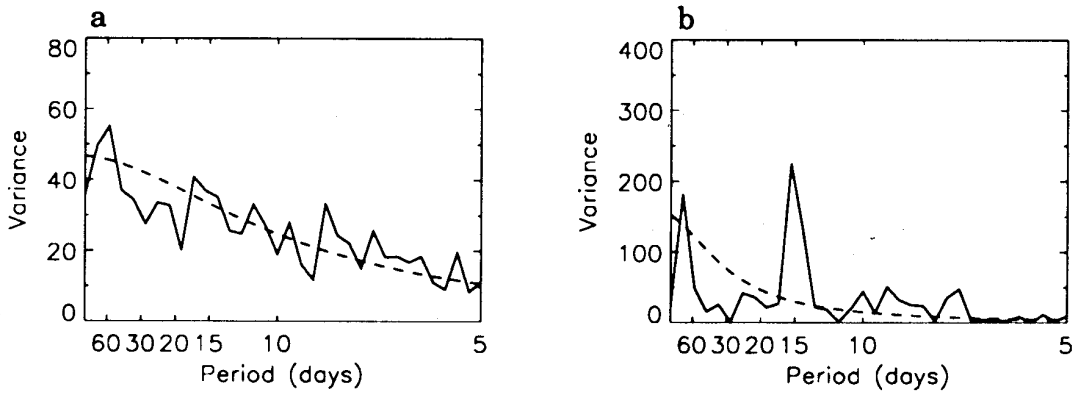

Fig. 14. (a) Mean of the spectra, and (b) spectrum of the mean for days 11 to 180 for July for the region of the SPCZ (150° E - 180° W, 15° S - 5° N).

frequencies. The Hovmoller diagram for days 121 to 180 for the SPCZ (Fig. 15) shows the coexistence of these differing scales quite well. Embedded in much larger scale and persistent regions of convection are small scale westward moving phenomena whose phase speed is about 5 m s^{-1}, typical for easterly waves. There is a tentative suggestion of an eastward propagation of the larger scale features, consistent with the analysis of Lau et al. (1991).

4. Discussion

This preliminary analysis of the variability of tropical convection in a high resolution version of the ECMWF model has revealed a rich tapestry of spatial and temporal scales. Preferred periodicities have been identified, ranging from 4 to 7 days typical of easterly waves, to 10 to 15 days observed in geostationary satellite data (Lau et al. 1991) and identified in the upper tropospheric equatorial winds (Yanai and Lu 1983), to 30 to 60 days characteristic of the intraseasonal oscillation. The model has displayed an interesting dependence of the variability on season. The synoptic scale high frequency waves with a well-defined periodicity are more prevalent in July. In January intraseasonal time scales dominate, with the synoptic scale events being more episodic in character. The dominance of intraseasonal periodicities in January is consistent with the observed tendency for the intraseasonal oscillation to be stronger during the northern hemisphere winter (Madden 1986).

It is very evident from the results described in this paper that the model's time

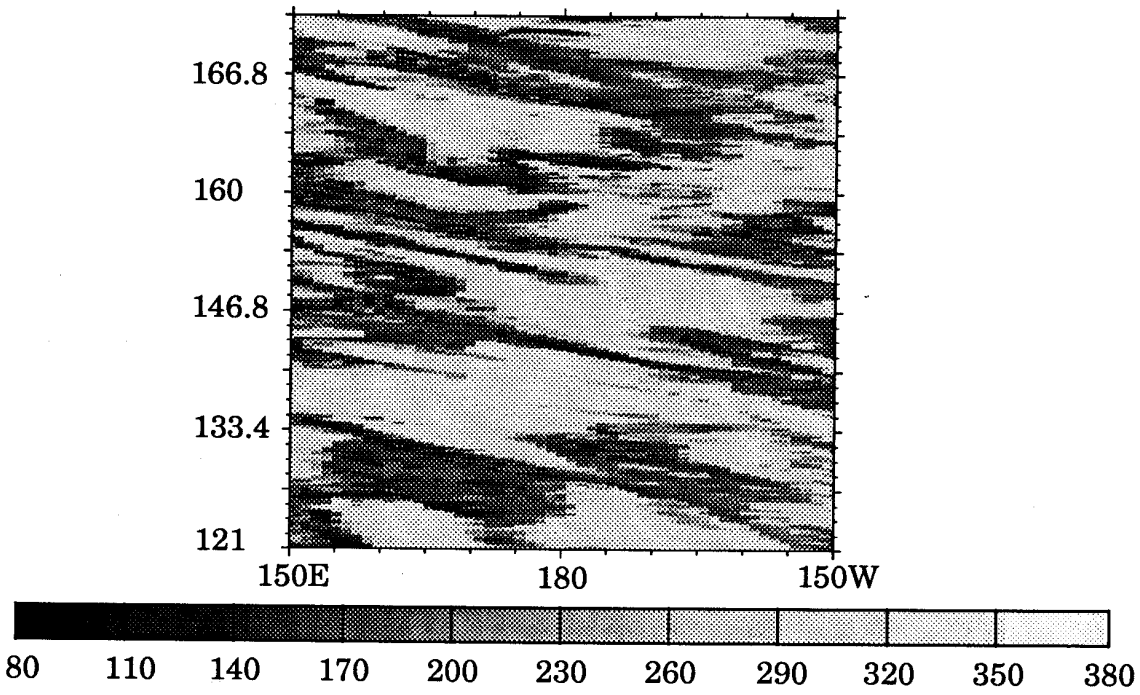

Fig. 15. Hovmoller diagram for days 121 to 180 of the OLR (W m^{-2}) along 10.7° S for July for the SPCZ sector 150° E to 150° W.

mean diabatic heating distribution in the tropics has a highly transient component which is not random, but shows synoptic scale organization with preferred periodicities. This result is important not only for in situ forecasting in the tropics, but also for the extratropics as well. In the tropics, the ability of a model to produce the correct spatial and temporal variability in convection is crucial to the prediction of tropical wave disturbances and their growth into tropical cyclones. It is encouraging that the model is able to simulate so many of the observed periodicities with the correct geographical location, particularly in July. However, the verification of the model's transience has been limited by the paucity of observational studies and the lack of information on interannual variability. It is hoped that the continuing increase in availability of satellite data and the comprehensive analysis of that data, such as proposed by Salby et al. (1991), will provide new insights into the temporal and spatial characteristics of tropical convection.

The tropical circulation cannot be seen in isolation; the interaction with the extratropics needs to be considered, in which the transient behavior of the tropical

heating may be crucially important. For instance, it has been suggested that variations in the diabatic heating over the warm pool associated with the intraseasonal oscillation (or 30- to 60-day wave) may induce a far-field response in the extratropics (Weickmann et al. 1985; Ferranti et al. 1990). On a shorter time scale, the direct migration of tropical disturbances poleward and their translation into, or their influence on, baroclinic waves in the extratropical storm tracks is another method by which the tropics influence the extratropics. Clearly, the ability of a model to generate tropical disturbances could have a substantial impact on this process; a study of this and its sensitivity to the model's convective parameterization is currently in progress.

The interaction between the tropics and the extratropics is a two way process in which the extratropics may in turn influence the tropical transience. Hsu et al. (1990) have suggested, for example, that the intraseasonal oscillation may be initiated by an extratropical wave train. Similarly, Zangvil and Yanai (1980) have hypothesized that the easterly waves in the equatorial Pacific may be excited by incursions of mid-latitude upper tropospheric troughs. The model results described in this paper are suggestive of a selection process, possibly indicative of extratropical influences, which transforms the highly periodic waves of the east Pacific and east Atlantic into episodic events farther west. Thus, the role of the extratropics in determining the nature of the transience in the tropics will form part of a subsequent study with the model.

Lau et al. (1991) and Weickmann and Khalsa (1990) both show evidence of westward moving cloud clusters embedded in an eastward moving super cluster, i.e. westward phase velocity and eastward group velocity. It is not clear at this stage how these two scales interact. For instance, Yamazaki and Murakami (1989) suggest that the amplitude of the tropical easterly waves is modulated with a quasi-monthly periodicity, and that this modulation may be associated with periods favorable to tropical cyclone genesis and/or development. Whether such a coupling of these differing spatial and temporal scales occurs in the model and whether it is important in determining the high and/or low frequency transience needs to be investigated. An interesting result of this study is the apparent long period variation in wave activity in the model, for example, over the east Pacific in July. This might be an artifact of running the model in perpetual mode and thus be associated with the long term drift of the land surface conditions, such as soil moisture. Nevertheless, this long term variability might have implications for the sampling period required in climate studies. Similarly, the existence of these highly periodic waves has implications also for

the frequency of sampling. The analysis described in this paper has been based on perpetual month integrations. Future studies will use seasonal cycle results and will also consider the interannual variation in the tropical transience, with and without interannual variations in sea surface temperatures.

5. Conclusions

This paper describes the results of a pilot study to investigate the variability of the simulated OLR in a general circulation model, and to compare it with the observed transience from satellite data and surface observations. The spatial and temporal sampling of the model is close to that for geostationary satellites and is adequate for studying both the intra- and inter-diurnal variability.

Results from the analysis of the intradiurnal variation suggest that the model is capable of representing the phase and amplitude of the diurnal harmonic with some success. Over the equatorial oceans a coherent diurnal cycle in the OLR is produced due to changes in the cloud cover. As expected, over land the phase of the diurnal cycle is dramatically different between clear and convective regions.

At interdiurnal time scales, the model displays both synoptic and low frequency variability which in many instances agrees well with observations. At synoptic frequencies, westward moving phenomena are identified whose periodicity and phase velocity are reasonable. The development of periodic easterly waves is most prevalent during the northern hemisphere summer. In January, the synoptic frequency variability associated with westward moving features is episodic rather than periodic in nature. However, the low frequency variability, which is also large particularly in the convectively active regions of the eastern hemisphere, has in contrast well defined periodicities, some in excess of 30 days representative of intraseasonal time scales. The fact that the spectrum of the mean also displays these low frequency peaks indicates that this periodicity is associated with variations on a large spatial scale.

This study has considered the variability in the OLR and hence, by implication, the convective activity. Many questions remain to be answered, such as the structure of the disturbances, their generation and dissipation mechanisms, their interaction with the extratropics and hence their role in the global circulation.

Acknowledgement. This work was performed under the auspices of the U.S. Department of Energy Environmental Sciences Division at the Lawrence Livermore National Laboratory under contract W-7405-ENG-48.

REFERENCES

Albright, M. D., E. Recker, R. J. Reed and R. Dang, 1985: The diurnal variation of deep convection and inferred precipitation in the central tropical Pacific during January - February 1979. *Mon. Wea. Rev.*, 113, 1663-1680.

Alexander, R. C., and R. L. Mobley, 1976: Monthly average sea-surface temperature and ice-pack limits on a 1° global grid. *Mon. Wea. Rev.*, 104, 143-148.

Burpee, R. W., 1972: The origin and structure of easterly waves in the lower troposphere of North Africa. *J. Atmos. Sci.*, 29, 77-90.

Burpee, R. W., 1974: Characteristics of north African easterly waves during the summers of 1968 and 1969. *J. Atmos. Sci.*, 31, 1556-1570.

Chang, C. P., V. F. Morris and J. M. Wallace, 1970: A statistical study of easterly waves in the western Pacific: July - December 1964. *J. Atmos. Sci.*, 27, 195-201.

Chang, C. P., T. Erikson and K. Lav, 1979: Northeasterly cold surges and near-equatorial disturbances over the winter MONEX area during December 1974. Part I: Synoptic aspects. *Mon. Wea. Rev.*, 107, 812-824.

Duvel, J. P., 1988: Analysis of diurnal, interdiurnal and interannual variations during northern hemisphere summers using METEOSAT infrared channels. *J. Clim.*, 1, 471-484.

Duvel, J. P., 1990: Convection over tropical Africa and Atlantic Ocean during northern summer. Part II: Modulation by easterly waves. *Mon. Wea. Rev.*, 118, 1855-1868.

Ferranti, L., T. N. Palmer, F. Molteni and E. Klinker, 1990: Tropical-extratropical interaction associated with the 30-60 day oscillation and its impact on medium and extended range prediction. *J. Atmos. Sci.*, 47, 2177-2199.

Fu, R., A. D. Del Genio and W. B. Rossow, 1990: Behavior of deep convective clouds in the tropical Pacific deduced from ISCCP radiances. *J. Clim.*, 3, 1129-1152.

Gill, A. E., 1980: Some simple solutions for heat-induced tropical circulation. *Q. J. R. Meteor. Soc.*, 106, 447-462.

Gray, W. M., and R. W. Jacobson, 1977: Diurnal variation of deep cumulus convection. *Mon. Wea. Rev.*, 105, 1171-1188.

Hartmann, D. L., and B. Liebmann, 1984: An observational study of tropical-midlatitude interaction on intraseasonal time scales during winter. *J. Atmos. Sci.*, 41, 3333-3350.

Hartmann, D. L., and E. E. Recker, 1986: Diurnal variation of outgoing longwave radiation in the tropics. *J. Clim. Appl. Meteor.*, 25, 800-812.

Hayashi, Y., 1974: Spectral analysis of tropical disturbances appearing in a GFDL general circulation model. *J. Atmos. Sci.*, 31, 180-218.

Hendon, H. H., and B. Liebmann, 1990: A composite study of onset of the Australian summer monsoon. *J. Atmos. Sci.*, 47, 2227-2240.

Holton, J. R., 1972: Waves in the equatorial stratosphere generated by tropospheric heat sources. *J. Atmos. Sci.*, 29, 368-375.

Hoskins, B. J. and D. Karoly, 1981: The steady linear response of a spherical atmosphere to thermal and orographic forcing. *J. Atmos. Sci.*, 38, 1179-1196.

Hsu, H., B. J. Hoskins and F. Jin, 1990: The 1985/86 intraseasonal oscillation and the role of the extratropics. *J. Atmos. Sci.*, 47, 823-839.

Lau, K-H., and N-C. Lau, 1990: Observed structure and propagation characteristics of tropical summertime synoptic scale disturbances. *Mon. Wea. Rev.*, 118, 1888-1913.

Lau, K. M., and P. H. Chan, 1985: Aspects of the 40-50 day oscillation during the northern winter as inferred from outgoing longwave radiation. *Mon. Wea. Rev.*, 113,1889-1909.

Lau, K. M., T. Nakazawa and C. H. Sui, 1991: Observations of cloud cluster hierarchies over the tropical western Pacific. *J. Geophys. Res.*, 96, 3197-3208.

Liebmann, B., and H. H. Hendon, 1990: Synoptic-scale disturbances near the equator. *J. Atmos. Sci.*, 47, 1463-1479.

Madden, R. A., 1986: Seasonal variations of the 40-50 day oscillation in the tropics. *J. Atmos. Sci.*, 43, 3138-3158.

Meisner, B. N., and P. A. Arkin, 1987: Spatial and annual variations in the diurnal cycle of large-scale tropical convective cloudiness and precipitation. *Mon. Wea. Rev.*, 115, 2009-2032.

Miller, M. J., A. C. M. Beljaars and T. N. Palmer, 1992: The sensitivity of the ECMWF model to the parameterization of evaporation from the tropical oceans. *J. Clim.*, in press.

Minnis, P., and E. F. Harrison, 1984: Diurnal variability of regional cloud and clear-sky radiative parameters derived from GOES data. Part III: November 1978 radiative parameters. *J. Clim. Appl. Meteor.*, 23, 1032-1051.

Morcrette, J.-J., 1990: Impact of changes to the radiation transfer parameterizations plus cloud optical properties in the ECMWF model. *Mon. Wea. Rev.*, 118, 847-873.

Morcrette, J.-J., 1991a: Radiation and cloud radiative properties in the ECMWF operational weather forecast model. *J. Geophys. Res.*, 96D, 9121-9132.

Morcrette, J.-J., 1991b: Evaluation of model-generated cloudiness: Satellite-observed

and model-generated diurnal variability of brightness temperature. *Mon. Wea. Rev.*, 119, 1205-1224.

Nitta, T., 1972: Structure of wave disturbances over the Marshall Islands during the years of 1956 and 1958. *J. Meteor. Soc. Japan*, 50, 85-103.

Nitta, T., Y. Nakagomi, Y. Suzuki, N. Hasegawa and A. Kadokura, 1985: Global analysis of the lower tropospheric disturbances in the tropics during the northern summer of the FGGE year. Part I: Global features of the disturbances. *J. Meteor. Soc. Japan*, 63, 1-18.

Reed, R. J., and E. E. Recker, 1971: Structure and properties of synoptic wave disturbances in the equatorial western Pacific. *J. Atmos. Sci.*, 28, 1117-1133.

Reed, R. J., D. C. Norquist and E. E. Recker, 1977: The structure and properties of African wave disturbances as observed during Phase III of GATE. *Mon. Wea. Rev.*, 105, 317-333.

Rui, H. and B. Wang, 1990: Development characteristics and dynamic structure of tropical intraseasonal convection anomalies. *J. Atmos. Sci.*, 47, 357-379.

Saha, K. F., F. Sanders and J. Shukla, 1981: Westward propagating predecessors of monsoon depressions. *Mon. Wea. Rev.*, 109, 330-344.

Salby, M. L., H. H. Hendon, K. Woodberry and K. Tanaka, 1991: Analysis of global cloud imagery from multiple satellites. *Bull. Amer. Meteor. Soc.*, 72, 467-480.

Simmons, A. J., 1982: The forcing of stationary wave motion by tropical diabatic heating. *Q. J. R. Meteor. Soc.*, 108, 503-534.

Simmons, A. J., D. M. Burridge, M. Jarraud, C. Girard and W. Wergen, 1988: The ECMWF medium-range prediction models. Development of the numerical formulations and the impact of increased resolution. *Meteor. Atmos. Phys.*, 40, 28-60.

Slingo, A., R. C. Wilderspin and S. J. Brentnall, 1987: Simulation of the diurnal cycle of outgoing longwave radiation with an atmospheric GCM. *Mon. Wea. Rev.*, 115, 1451-1457.

Slingo, J. M., 1987: The development and verification of a cloud prediction scheme for the ECMWF model. *Q. J. R. Meteor. Soc.*, 113, 899-928.

Tai, K. S., and Y. Ogura, 1987: An observational study of easterly waves over the eastern Pacific in the northern summer using FGGE data. *J. Atmos. Sci.*, 44, 339-361.

Tiedtke, M., 1989: A comprehensive mass-flux scheme for cumulus parameterization in large-scale models. *Mon. Wea. Rev.*, 117, 1779-1800.

Tiedtke, M., W. A. Heckley and J. M. Slingo, 1988: Tropical forecasting at ECMWF: The influence of physical parametrization on the mean structure of forecasts and analyses. *Q. J. R. Meteor. Soc.*, 114, 639-664.

Wallace, J. M., and M. L. Blackmon, 1983: Observations of low-frequency atmospheric variability. In *Large-scale Dynamical Processes in the Atmosphere*. Eds. B. J. Hoskins and R. P Pearce, Academic Press, pp. 55-94.

Wallace, J. M., and C. P. Chang, 1969: Spectrum analysis of large-scale wave disturbances in the tropical lower troposphere. J. Atmos. Sci., 26, 1010-1025.

Wallace, J. M., and D. Gutzler, 1981: Teleconnections in the geopotential height field during the northern hemisphere winter. *Mon. Wea. Rev.*, 109, 785-812.

Webster, P. J., 1983: Large-scale structure of the tropical atmosphere. In *Large-scale Dynamical Processes in the Atmosphere.* Eds. B. J. Hoskins and R. P. Pearce, Academic Press, pp. 235-275.

Weickmann, K. M., and S. J. S. Khalsa, 1990: The shift of convection from the Indian Ocean to the western Pacific Ocean during a 30-60 day oscillation. *Mon. Wea.*

Rev., 118, 964-978.

Weickmann, K. M., G. R. Lussky and J. E. Kutzbach, 1985: Intraseasonal (30-60 day) fluctuations of outgoing longwave radiation and 250mb streamfunction during northern winter. *Mon. Wea. Rev.*, 113, 941-961.

Yanai, M., and Y. Hayashi, 1969: Large-scale equatorial waves penetrating from the upper troposphere into the lower stratosphere. *J. Meteor. Soc. Japan*, 47, 167-182.

Yanai, M., and M-M. Lu, 1983: Equatorially trapped waves at the 200mb level and their association with meridional convergence of wave energy flux. *J. Atmos. Sci.*, 40, 2785-2803.

Yamazaki, N., and M. Murakami, 1989: An intraseasonal amplitude modulation of the short-term tropical disturbances over the Western Pacific. *J. Meteor. Soc. Japan*, 67, 791-807.

Yanai, M., T. Maruyama, T. Nitta and Y. Hayashi,1968: Power spectra of large-scale disturbances over the tropical Pacific. *J. Meteor. Soc. Japan*, 46, 308-323.

Zangvil, A., and M. Yanai, 1980: Upper tropospheric waves in the tropics. Part I: Dynamical analysis in the wavenumber-frequency domain. *J. Atmos. Sci.*, 37, 283-298.

Zangvil, A., and M. Yanai, 1981: Upper tropospheric waves in the tropics. Part II: Association with clouds in the wavenumber-frequency domain. *J. Atmos. Sci.*, 38, 939-953.

Zwiers, F. W., and G. J. Boer, 1987: A comparison of climates simulated by a general circulation model when run in the annual cycle and perpetual modes. *Mon. Wea. Rev.*, 115, 2626-2644.